Cell

Sequence-Dependent Sorting of Recycling Proteins by Actin-Stabilized Endosomal Microdomains

Manojkumar A. Puthenveedu,[1,*] Benjamin Lauffer,[2] Paul Temkin,[2] Rachel Vistein,[1] Peter Carlton,[3] Kurt Thorn,[4] Jack Taunton,[5] Orion D. Weiner,[4] Robert G. Parton,[6] and Mark von Zastrow[2,5]
[1]Department of Biological Sciences, Carnegie Mellon University, Pittsburgh, PA, USA
[2]Department of Psychiatry
[3]Department of Physiology
[4]Department of Biochemistry and Biophysics
[5]Department of Cellular and Molecular Pharmacology
University of California at San Francisco, San Francisco, CA 94158, USA
[6]The University of Queensland, Institute for Molecular Bioscience and Centre for Microscopy and Microanalysis, St. Lucia, Queensland 4072, Australia 8
*Correspondence: map3@andrew.cmu.edu
DOI 10.1016/j.cell.2010.10.003

SUMMARY

The functional consequences of signaling receptor endocytosis are determined by the endosomal sorting of receptors between degradation and recycling pathways. How receptors recycle efficiently, in a sequence-dependent manner that is distinct from bulk membrane recycling, is not known. Here, in live cells, we visualize the sorting of a prototypical sequence-dependent recycling receptor, the beta-2 adrenergic receptor, from bulk recycling proteins and the degrading delta-opioid receptor. Our results reveal a remarkable diversity in recycling routes at the level of individual endosomes, and indicate that sequence-dependent recycling is an active process mediated by distinct endosomal subdomains distinct from those mediating bulk recycling. We identify a specialized subset of tubular microdomains on endosomes, stabilized by a highly localized but dynamic actin machinery, that mediate this sorting, and provide evidence that these actin-stabilized domains provide the physical basis for a two-step kinetic and affinity-based model for protein sorting into the sequence-dependent recycling pathway.

INTRODUCTION

Cells constantly internalize a large fraction of proteins from their surface and the extracellular environment. The fates of these internalized proteins in the endosome have a direct impact on several critical functions of the cell, including its response to environmental signals (Lefkowitz et al., 1998; Marchese et al., 2008; Sorkin and von Zastrow, 2009).

Internalized proteins have three main fates in the endosome. First, many membrane proteins, such as the transferrin receptor (TfR), are sorted away from soluble proteins, largely by bulk membrane flow back to the cell surface. This occurs via the formation and fission of narrow tubules that have a high ratio of membrane surface area (and therefore membrane proteins) to volume (soluble contents) (Mayor et al., 1993). Several proteins have been implicated in the formation of these tubules (Shinozaki-Narikawa et al., 2006; Cullen, 2008; Traer et al., 2007), which provide a geometric basis to bulk recycling and explain how nutrient receptors can recycle leaving soluble nutrients behind to be utilized in the lysosome (Dunn and Maxfield, 1992; Mayor et al., 1993; Maxfield and McGraw, 2004). Second, many membrane proteins are transported to the lysosome to be degraded. This involves a process called involution, where proteins are packaged into vesicles that bud off to the interior of the endosome and, in essence, converts these proteins into being a part of the soluble contents (Piper and Katzmann, 2007). Involution has also been studied extensively, and the machinery responsible, termed ESCRT complex, identified (Hurley, 2008; Saksena et al., 2007; Williams and Urbé, 2007). Third, several other membrane proteins, such as many signaling receptors, escape the bulk recycling and degradation pathways, and are instead recycled in a regulated manner (Hanyaloglu and von Zastrow, 2008; Yudowski et al., 2009). This requires a specific *cis*-acting sorting sequence present on the receptor's cytoplasmic surface (Cao et al., 1999; Hanyaloglu and von Zastrow, 2008). How receptors use these sequences to escape the involution pathway and recycle, though they are excluded from the default recycling pathway (Maxfield and McGraw, 2004; Hanyaloglu et al., 2005), is a fundamental cell biological question that is still unanswered.

Although it is clear that different recycling cargo can travel through discrete endosomal populations (Maxfield and McGraw, 2004), endosome-to-plasma membrane recycling from a single endosome is generally thought to occur via a uniform population of tubules. Contrary to this traditional view, we identify specialized endosomal tubular domains mediating sequence-dependent recycling that are kinetically and biochemically distinct

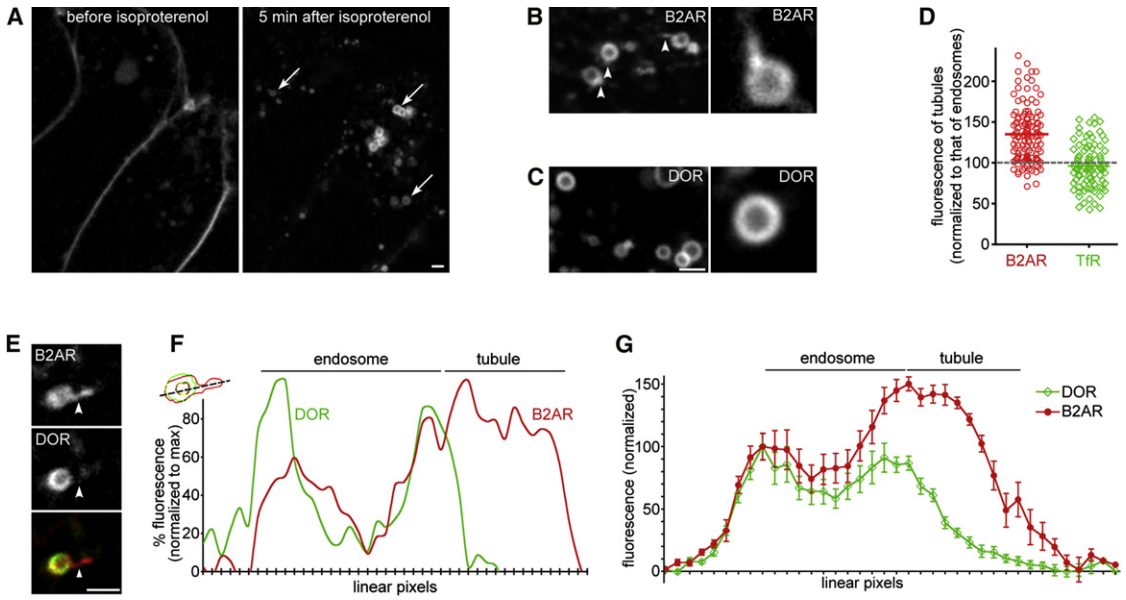

Figure 1. B2AR Is Enriched in Endosomal Tubular Domains Devoid of DOR

(A) HEK293 cells stably expressing FLAG-B2AR, labeled with fluorescently-tagged anti-FLAG antibodies, were followed by live confocal imaging before (left) and after 5 min (right) of isoproterenol treatment. Arrows show internal endosomes.

(B) Example endosomes showing tubular domains enriched in B2AR (arrowheads) with one enlarged in the inset.

(C) Examples of DOR endosomes. DOR is smoothly distributed on the endosomal membrane and is not detected in tubules.

(D) Average fluorescence of B2AR (red circles) and TfR (green diamonds) calculated across multiple tubules (n = 123 for B2AR, 100 for TfR). B2AR shows a 50% enrichment over the endosomal membrane, while TfR is not enriched. Each point denotes an individual tubule, the bar denotes the mean, and the gray dotted line denotes the fluorescence of the endosomal membrane.

(E) An endosome containing both internalized B2AR and DOR, showing a tubule containing B2AR but no detectable DOR (arrowheads).

(F) Trace of linear pixel values across the same endosome, normalized to the maximum, confirms that the tubule is enriched for B2AR but not DOR.

(G) Linear pixel values of endosomal tubules averaged across 11 endosomes show specific enrichment of B2AR in tubules.

Error bars are SEM. See also Figure S1 and Movie S1 and Movie S2.

from the domains that mediate bulk recycling. These domains are stabilized by a local actin cytoskeleton that is required and sufficient for receptor recycling. We propose that such specialized actin-stabilized domains provide the physical basis for overcoming a kinetic barrier for receptor entry into endosomal tubules and for affinity-based concentration of proteins in the sequence-dependent recycling pathway.

RESULTS

Visualization of Receptor Sorting in the Endosomes of Living Cells

The beta 2-adrenergic receptor (B2AR) and the delta opioid receptor (DOR) provide excellent models for physiologically relevant proteins that are sorted from each other in the endosome. Although they share endocytic pathways, B2AR is recycled efficiently in a sequence-dependent manner while DOR is selectively degraded in the lysosome (Cao et al., 1999; Whistler et al., 2002). To study the endosomal sorting of these cargo molecules, we started by testing whether tubulation was involved in this process. Because such sorting has not been observed in vivo, we first attempted to visualize the dynamics of receptor sorting in live HEK293 cells expressing fluorescently labeled B2AR or DOR receptors, using high-resolution confocal microscopy. Both receptors were observed mostly on the cell surface before isoproterenol or DADLE, their respective agonists, were added. After agonist addition, both B2AR (Figure 1A) and DOR (data not shown) were robustly internalized, and appeared in endosomes within 5 min (Figure 1A and Movie S1 available online). As a control, receptors did not internalize in cells not treated with agonists, but imaged for the same period of time (Figure S1A). The B2AR-containing endosomes colocalized with the early endosome markers Rab5 (Figure S1B) and EEA1 (data not shown), consistent with previous data.

Internalized B2AR (Figure 1B), but not DOR (Figure 1C), also labeled tubules that extended from the main body of the receptor. When receptor fluorescence was quantified across multiple B2AR-containing tubules, we saw that receptors were enriched in these tubules compared to the rest of the endosomal limiting membrane (Figure 1D). The bulk recycling protein TfR, in contrast, was not enriched in endosomal tubules (Figure 1D). This suggests that sequence-dependent recycling receptors are enriched by an active mechanism in these endosomal tubules.

These endosomal tubules were preferentially enriched for B2AR over DOR on the same endosome. In cells coexpressing FLAG-tagged B2AR and GFP-tagged DOR, we observed endosomes that contained both receptors within 5 min after coapplying isoproterenol and DADLE. Notably, these endosomes extruded tubules that contained B2AR but not detectable DOR

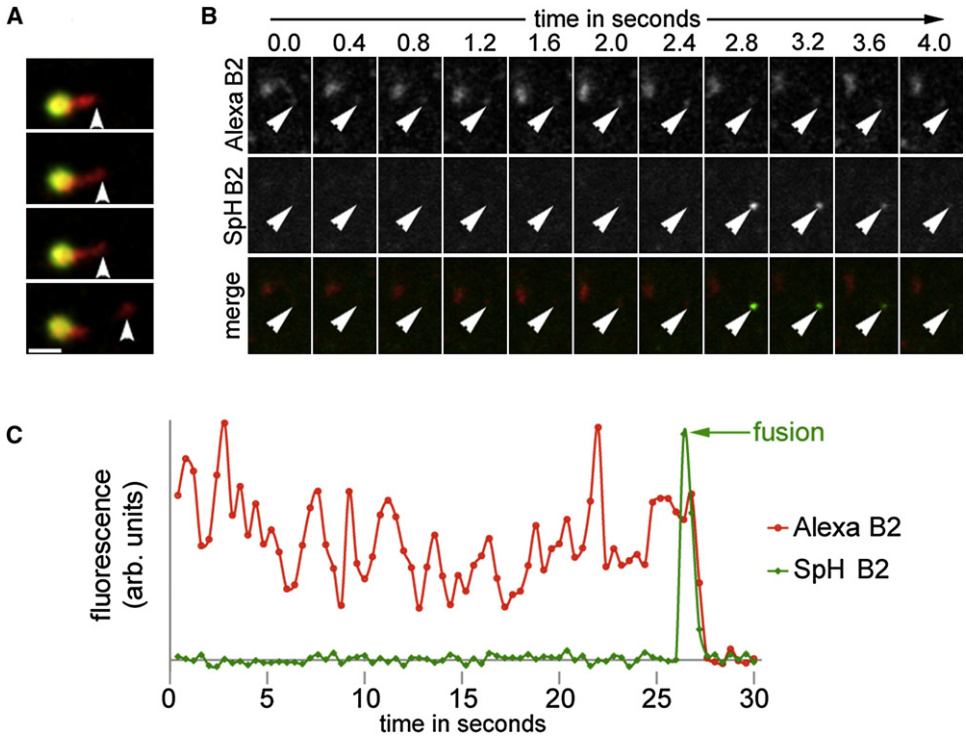

Figure 2. Membranes Derived from Endosomal Tubules Deliver B2AR to the Cell Surface

(A) Frames from a representative time lapse series showing scission of a vesicle that contains B2AR but not detectable DOR, from an endosomal tubule.

(B) An image plane close to the plasma membrane in cells coexpressing SpH-B2AR and FLAG-B2AR (labeled with Alexa555), exposed to isoproterenol for 5 min, and imaged by fast dual-color confocal microscopy. Arrows denote the FLAG-B2AR-containing membrane derived from the endosomal tubule that fuses.

(C) Fluorescence trace of the B2AR-containing membranes from the endosome in movie S4, showing the spike in SpH-B2AR fluorescence (fusion) followed by rapid loss of fluorescence.

Scale bars represent 1μm. See also Figure S1 and Movie S3 and Movie S4.

(e.g., in Figure 1E and in Movie S2). Fluorescence traces across the endosome and the tubule confirmed that DOR was not detectable in these B2AR tubules, suggesting that B2AR was specifically sorted into these tubular domains (e.g., in Figure 1F). When linear pixel values from multiple sorting events were quantified, B2AR was enriched ~50% in the endosomal domains from which tubules originate, compared to the endosomal membrane outside these domains (Figure 1G). Thus, these experiments resolve, for the first time, individual events that mediate sorting of two signaling receptors in the endosomes of live cells.

B2AR-Containing Endosomal Tubules Deliver Receptors to the Cell Surface

To test whether these tubules mediated recycling of B2AR, we visualized direct delivery of receptors from these tubules to the cell surface. In endosomes containing internalized B2AR and DOR, these tubular domains pinched off vesicles that contained B2AR but not detectable levels of DOR (Figure 2A and Movie S3). To reliably assess if these vesicles traveled to the surface and fused with the plasma membrane, we combined our current imaging with a method that we have used previously to visualize individual vesicle fusion events mediating surface receptor delivery (Yudowski et al., 2006). Briefly, we attached the pH-sensitive GFP variant superecliptic pHluorin to the extracellular domain of B2AR (SpH-B2AR) (Miesenböck et al., 1998). SpH-B2AR is highly fluorescent when exposed to the neutral pH at the cell surface, but is quenched in the acidic environments of endosomes and intracellular vesicles. This allows the detection of individual fusion events of vesicles containing B2AR at the cell surface (Yudowski et al., 2009). In cells coexpressing SpH-B2AR and B2AR labeled with a pH-insensitive fluorescent dye (Alexa-555), vesicles derived from the endosomal tubules trafficked to the cell surface and fused, as seen by a sudden increase in SpH fluorescence followed by loss of fluorescence due to diffusion (Figure 2B, and Movie S4). A fluorescence trace from movie S4 confirmed the fusion and loss of B2AR fluorescence (Figure 2C). Also, Rab4 and Rab11, which function in endosome-to-plasma membrane recycling (Zerial and McBride, 2001; Maxfield and McGraw, 2004), were localized to the domains containing B2AR (Figure S1). Together, this indicates that the B2AR-containing endosomal tubules mediate delivery of B2AR to the cell surface.

B2AR-Containing Tubules Are Marked by a Highly Localized Actin Cytoskeleton

We next examined whether the B2AR-containing microdomains were biochemically distinct from the rest of the endosomal membrane. We first focused on actin, as the actin cytoskeleton

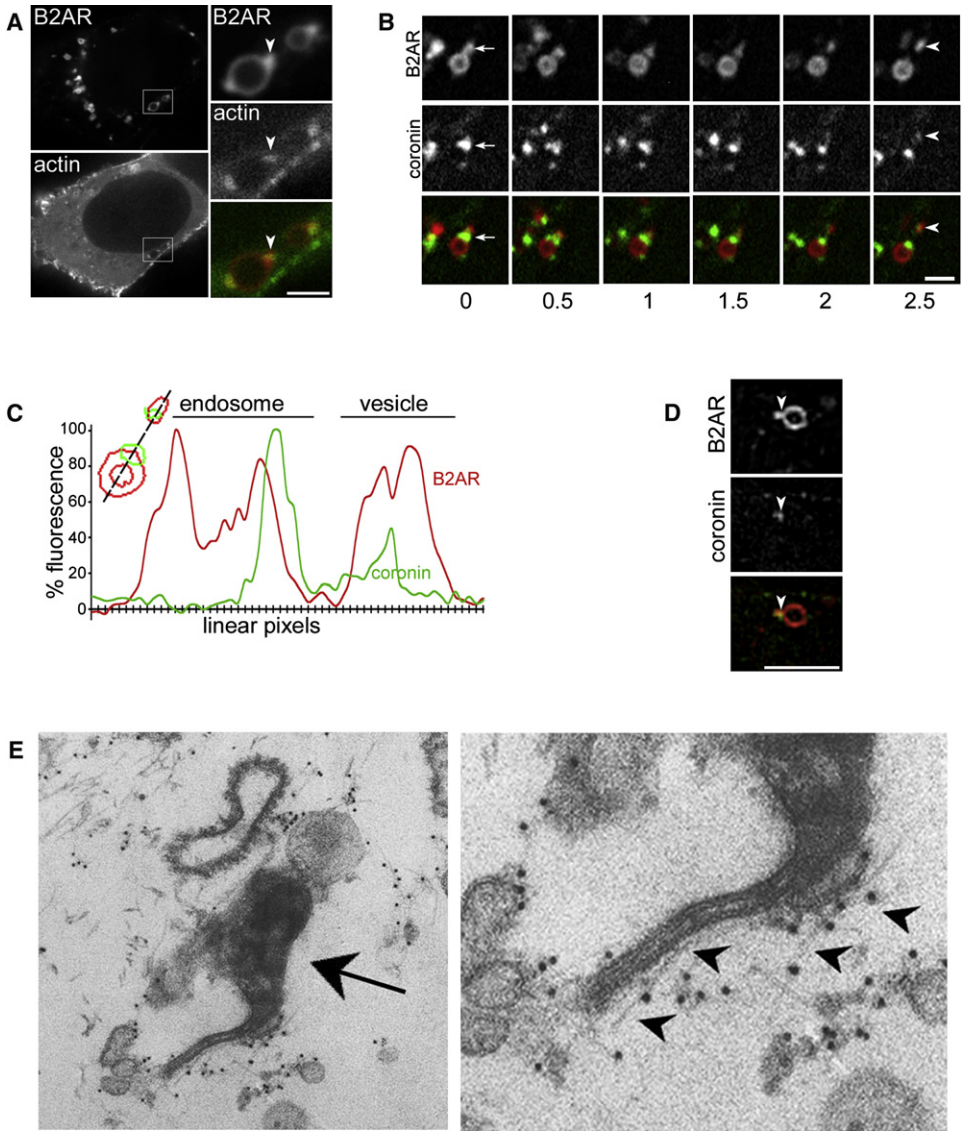

Figure 3. B2AR Tubules Are Marked by a Highly Localized Actin Cytoskeleton

(A) Cells coexpressing fluorescently labeled B2AR and actin-GFP exposed to isoproterenol for 5 min. The boxed area is enlarged in the inset, with arrowheads indicating specific concentration of actin on B2AR endosomal tubules.

(B) Time lapse series from an example endosome with B2AR and coronin-GFP. Coronin is detectable on the endosomal tubule (arrows) and on the vesicle (arrowheads) that buds off the endosome.

(C) A trace of linear pixel values across the same endosome, normalized to maximum fluorescence, shows coronin on the endosomal domain and the vesicle.

(D) Example structured illumination image of a B2AR endosome showing specific localization of coronin to a B2AR tubule (arrowheads).

(E) Electron micrograph of an HRP-positive endosome (arrow) showing actin filaments (labeled with 9 nm gold, arrowheads) along a tubule. The right panel shows an enlarged view.

See also Movie S5 and Movie S6.

is required for efficient recycling of B2AR but not of TfR (Cao et al., 1999; Gage et al., 2005), and as it has been implicated in endosome motility (Stamnes, 2002; Girao et al., 2008) and vesicle scission at the cell surface (Yarar et al., 2005; Perrais and Merrifield, 2005; Kaksonen et al., 2005). Strikingly, in cells coexpressing B2AR and actin-GFP, actin was concentrated on the endosome specifically on the tubular domains containing B2AR (Figure 3A). Virtually every B2AR tubule observed showed this specific actin concentration on the tubule (n = 350). As with actin, coronin-GFP (Uetrecht and Bear, 2006), an F-actin binding protein, also localized specifically to the B2AR-containing tubules on endosomes (Figure 3B), confirming that this was a polymerized actin cytoskeleton. Coronin was also observed on the B2AR-containing vesicle that was generated by dynamic scission of the B2AR tubule (Figure 3B and Movie S5). Fluorescence traces of the linear pixels across the tubule and the vesicle

confirmed that coronin pinched off with the B2AR vesicle (Figure 3C).

We also used two separate techniques to characterize actin localization on these tubules beyond the ~250 nm resolution offered by conventional microscopy. First, we first imaged the localization of coronin on endosomes containing B2AR tubules using structured illumination microscopy (Gustafsson et al., 2008), which resolves structures at ~100 nm spatial resolution. 3D stacks obtained using this high-resolution technique confirmed that coronin was specifically localized on the endosomal tubule that contained B2AR (Figure 3D and Movie S6). Second, we examined the morphology of actin on endosomal tubules at the ultrastructural level by pre-embedding immunoelectron microscopy. Actin was clearly labeled as filaments lying along tubules extruded from endosomal structures (Figure 3E).

Actin Is Dynamically Turned over on the B2AR-Containing Endosomal Tubules

We then tested whether the actin filaments on these tubules were a stable structure or were dynamically turned over. When cells expressing actin-GFP were exposed to latrunculin, a drug that prevents actin polymerization, endosomal actin fluorescence became indistinguishable from the "background" cytoplasmic fluorescence within 16–18 s after drug exposure (e.g., in Figure 4A). When quantified across multiple cells, endosomal actin fluorescence showed an exponential loss after latrunculin exposure, with a $t_{1/2}$ of 3.5 s (99% Confidence Interval = 3.0 to 4.1 s) (Figure 4B), indicating that endosomal actin turned over quite rapidly. As a control, stress fibers, which are composed of relatively stable capped actin filaments, were turned over more slowly in these same cells (e.g., in Figure S2A). Endosomal actin was lost in >98% of cells within 30 s after latrunculin, in contrast to stress fibers, which persisted for over 2 min in >98% of cells (Figure S2B). Rapid turnover of endosomal actin was also independently confirmed by fluorescence recovery after photobleaching (FRAP) studies. When a single endosomal actin spot was bleached, the fluorescence recovered rapidly within 20 s (Figure 4C). As a control for more stable actin filaments, stress fibers showed little recovery of fluorescence after bleaching in this interval (Figure 4C). Exponential curve fits yielding a $t_{1/2}$ of 8.26 s (99% CI = 7.65 to 8.97 s), consistent with rapid actin turnover (Figure 4D). In contrast, only part of the fluorescence (~30%) was recovered in stress fibers in the same cells by 20 s, with curve fits yielding a $t_{1/2}$ of 50.35 s (99% CI = 46.05 to 55.54 s). These results indicate that actin is dynamically assembled on the B2AR recycling tubules.

Considering the rapid turnover of actin, we next explored the machinery responsible for localizing actin at the tubule. The Arp2/3 complex is a major nucleator of dynamic actin polymerization that has been implicated in polymerization-based endosome motility (Stamnes, 2002; Girao et al., 2008; Pollard, 2007). Arp3, an integral part of the Arp2/3 complex useful for visualizing this complex in intact cells (Merrifield et al., 2004), was specifically concentrated at the base of the B2AR tubules on the endosome (e.g., in Figure 4E and fluorescence trace in Figure 4F, Movie S7). Every B2AR tubule observed had a corresponding Arp3 spot at its base (n = 200). Surprisingly, however, we did not see N-WASP and WAVE-2, canonical members of the two main families of Arp2/3 activators (Millard et al., 2004), on the endosome (Figure 4G). Similarly, we did not see endosomal recruitment of activated Cdc42, as assessed by a previously characterized GFP-fusion reporter consisting of the GTPase binding domain of N-WASP (Benink and Bement, 2005) (data not shown). All three proteins were readily detected at lamellipodia and filopodia as expected, indicating that the proteins were functional in these cells. While we cannot rule out a weak or transitory interaction of these activators with Arp2/3 at the endosome, the lack of enrichment prompted us to test for alternate Arp2/3 activators. Cortactin, an Arp- and actin- binding protein present on endosomes, has been proposed to be such an activator (Kaksonen et al., 2000; Millard et al., 2004; Daly, 2004). Cortactin-GFP was clearly concentrated at the base of the B2AR tubule on the endosome (Figure 4G), in a pattern identical to Arp2/3. When quantified (>200 endosomes each), every B2AR tubule was marked by cortactin, while none of the endosomes showed detectable N-WASP, WAVE-2, or Cdc42. Similarly, the WASH protein complex, which has been recently implicated in trafficking from the endosome (Derivery et al., 2009; Gomez and Billadeau, 2009; Duleh and Welch, 2010), was also clearly localized to B2AR tubules (Figure 4G). Together, these data suggest that an Arp2/3-, cortactin- and WASH-based machinery mediates dynamic actin assembly on the endosome.

B2AR-Containing Tubules Are a Specialized Subset of Recycling Tubules on the Endosome

Since the traditional view is that the endosomal tubules that mediate direct recycling to the plasma membrane are a uniform population, we next tested whether these tubules were the same as those that recycle bulk cargo. When B2AR recycling was visualized along with bulk recycling of TfR, endosomes containing both cargo typically extruded three to four tubules containing TfR. Strikingly, however, only one of these contained detectable amounts of B2AR (Example in Figure 5A, quantified in Figure 5B). This was consistent with fast 3D confocal live cell imaging of B2AR in endosomes, which showed that most endosomes extruded only one B2AR containing tubule, with a small fraction containing two. When quantified, only 24.4% of all TfR tubules contained detectable B2AR (n = 358 tubules).

B2AR Tubules Are a Kinetically and Biochemically Distinct from Bulk Recycling Tubules

When the lifetimes of tubules were quantified, the majority (>80%) of B2AR tubules lasted more than 30 s. In contrast, the majority of TfR tubules devoid of B2AR lasted less than 30 s (Figures 5B and 5C, Movie S8). Each endosome extruded several tubules containing TfR, only a subset (~30%) of which were marked by actin, coronin, or cortactin (Figures 5D and 5E, arrows). Time-lapse movies indicated that the highly transient TfR-containing tubules were extruded from endosomal domains that were lacking cortactin (Figure 5E, arrows), while the relatively stable B2AR containing tubules were marked by cortactin (Figure 5E, arrowheads). Importantly, the relative stability of the subset of tubules was conferred by the actin cytoskeleton, as disruption of actin using latrunculin virtually abolished the stable fraction of TfR tubules (Figures 5B and 5C).

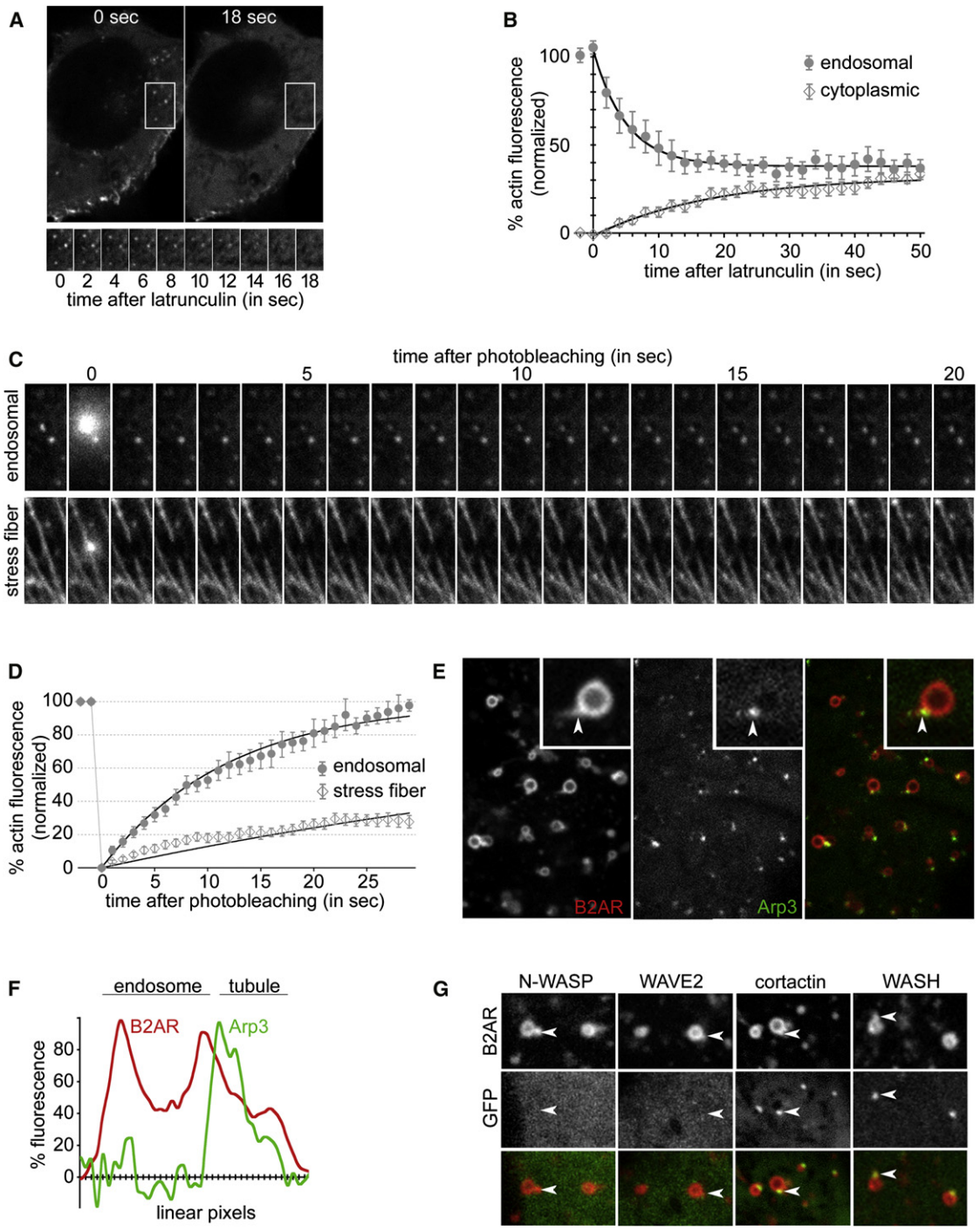

Figure 4. Actin on B2AR Tubules Is Dynamic and Arp2/3-Nucleated

(A) Cells expressing actin-GFP imaged live after treatment with 10 μM latrunculin for the indicated times, show rapid loss of endosomal actin. A time series of the boxed area, showing several endosomal actin loci, is shown at the lower panel.

(B) The change in endosomal and cytoplasmic actin fluorescence over time after latrunculin normalized to initial endosomal actin fluorescence (n = 10). One-phase exponential curve fits (solid lines) show a $t_{1/2}$ of 3.5 s for actin loss (R^2 = 0.984, d.f = 23, Sy.x = 2.1 for endosomal actin, R^2 = 0.960, d.f = 23, Sy.x = 1.9 for cytoplasmic). Endosomal and cytoplasmc actin fluorescence becomes statistically identical within 15 s after latrunculin. Error bars denote SEM.

(C) Time series showing FRAP of representative examples of endosomal actin (top) and stress fibers (bottom).

(D) Kinetics of FRAP of actin (mean ± s.e.m) quantified from 14 endosomes and 17 stress fibers. One-phase exponential curve fits (lines), show a $t_{1/2}$ of 8.26 s for endosomal actin (R^2 = 0.973, d.f = 34, Sy.x = 4.8) and 50.35 s for stress fibers (R^2 = 0.801, d.f = 34, Sy.x = 3.9).

Together, these results suggest that sequence-dependent recycling of B2AR is mediated by specialized tubules that are kinetically and biochemically distinct from the bulk recycling tubules containing only TfR.

A Kinetic Model for Sorting of B2AR into a Subset of Endosomal Tubules

The relative stability of B2AR tubules suggested a simple model, based on kinetic sorting, for how sequence-dependent cargo was sorted into a specific subset of tubules and excluded from the transient TfR-containing bulk-recycling tubules. We hypothesized that B2AR diffuses more slowly on the endosomal membrane relative to bulk recycling cargo. The short lifetimes of the bulk-recycling tubules would then create a kinetic barrier for B2AR entry, while this barrier would be overcome in the subset of tubules stabilized by actin.

To test the key prediction of this model, that B2AR diffuses more slowly than TfR on the endosomal membrane, we directly measured the diffusion rates of B2AR and TfR using FRAP. When B2AR or TfR was bleached on a small part of the endosomal membrane, B2AR fluorescence took significantly longer to recover than TfR (Figure 5F). When quantified, the rate of recovery of fluorescence of B2AR ($t_{1/2}$ = 25.77 s, 99% CI 23.45 to 28.6 s) was ~4 times slower than that of TfR ($t_{1/2}$ = 6.21 s, 99% CI 5.49 to 7.17 s), indicating that B2AR diffuses significantly slower on the endosomal membrane than TfR (Figures 5F and 5G). Neither B2AR or TfR recovered within the time analyzed when the whole endosome was bleached (Figure 5H), confirming that the recovery of fluorescence was due to diffusion from the unbleached part of the endosome and not due to delivery of new receptors via trafficking. Further, B2AR on the plasma membrane diffused much faster than on the endosome ($t_{1/2}$ = 6.45 s, 99% CI 5.62 to 7.66 s), comparable to TfR, suggesting that B2AR diffusion was slower specifically on the endosome (Figure 5H).

We next tested whether the diffusion of B2AR into endosomal tubules was slower than that of TfR, by using the rate of increase of B2AR fluorescence as an index of receptor entry into tubules. B2AR fluorescence continuously increased throughout the duration of the tubule lifetimes (Figure S3A). Further, in a single tubule containing TfR and B2AR, TfR fluorescence reached its maximum at a markedly faster rate than that of B2AR (Figure S3B). Together, these results suggest that slow diffusion of B2AR on the endosome and stabilization of recycling tubules by actin can provide a kinetic basis for specific sorting of sequence-dependent cargo into subsets of endosomal tubules.

Local Actin Assembly Is Required for B2AR Entry into the Subset of Tubules

Because actin stabilizes the B2AR-containing subset of tubules, the model predicts that endosomal actin would be required for sequence-dependent concentration of B2AR into these tubules. Consistent with this, B2AR was no longer concentrated in endosomal tubules when endosomal actin was acutely removed using latrunculin (e.g., in Figure 6A). When the pixel fluorescence along the limiting membrane of multiple endosomes was quantified, B2AR was distributed more uniformly along the endosomal membrane in the absence of actin (Figures 6B and 6C). We further confirmed this by comparing the variance in B2AR fluorescence along the endosomal perimeter, irrespective of their orientation. B2AR fluorescence was significantly more uniform in endosomes without actin (Figure 6D), indicating that actin was required for endosomes to concentrate B2AR in microdomains. Less than 20% of endosomes showed B2AR-containing tubules in the absence of endosomal actin, in contrast to control cells where over 75% of endosomes showed B2AR-containing tubules (Figure 6E). Further, cytochalasin D, a barbed-end capping drug that prevents further actin polymerization but does not actively cause depolymerization, also inhibited B2AR entry into tubules (Figure 6E) and B2AR surface recycling (Figure S4A). Neither TfR tubules on endosomes (Figure 6E) nor TfR recycling (Figure S4B) was inhibited by actin depolymerization, consistent with a role for actin specifically in sequence-dependent recycling of B2AR (Cao et al., 1999). Further, depletion of cortactin using siRNA (Figure 6F) also inhibited B2AR entry into tubules (Figures 6G and 6H). This inhibition was specific to cortactin depletion, as it was rescued by exogenous expression of cortactin (Figure 6H). Together, these results indicate that a localized actin cytoskeleton concentrates sequence-dependent recycling cargo into a specific subset of recycling tubules on the endosome.

B2AR Sorting into the Recycling Subdomains Is Mediated by Its C-Terminal PDZ-Interacting Domain

We next asked whether this actin-dependent concentration of receptors into endosomal tubules depended on the PDZ-interacting sequence present in the B2AR cytoplasmic tail that mediates sequence-dependent recycling (Cao et al., 1999; Gage et al., 2005). To test if the sequence was required, we used a mutant B2AR (B2AR-ala) in which the recycling sequence was specifically disrupted by the addition of a single alanine (Cao et al., 1999). Unlike B2AR, internalized B2AR-ala was not able to enter the tubular domains in the endosome (e.g., in Figure 6I, quantified in Figure 6J), or recycle to the cell surface (Figure S4). To test if this sequence was sufficient, we used a chimeric DOR construct with the B2AR-derived recycling sequence fused to its cytoplasmic tail, termed DOR-B2 (Gage et al., 2005), which recycles much more efficiently than DOR (Figure S4). In contrast to DOR, which showed little concentration in endosomal tubules, DOR-B2 entered tubules (Figures 6I and 6J) and recycled in an actin-dependent manner similar to B2AR (Figure S4D). Together, these results indicate that the

(E) Example endosomes in live cells coexpressing B2AR and Arp3-GFP showing Arp3 at the base of B2AR tubules (arrowhead in the inset).
(F) Trace of linear pixel fluorescence of B2AR and Arp3 shows Arp3 specifically on the endosomal tubule.
(G) Example endosomes from cells coexpressing B2AR and N-WASP-, WAVE2-, cortactin-, or WASH-GFP. N-WASP and WAVE2 were not detected on endosomes, while cortactin and WASH were concentrated at the B2AR tubules (arrowheads).
Scale bars represent 1 μm. See also Figure S2 and Movie S7.

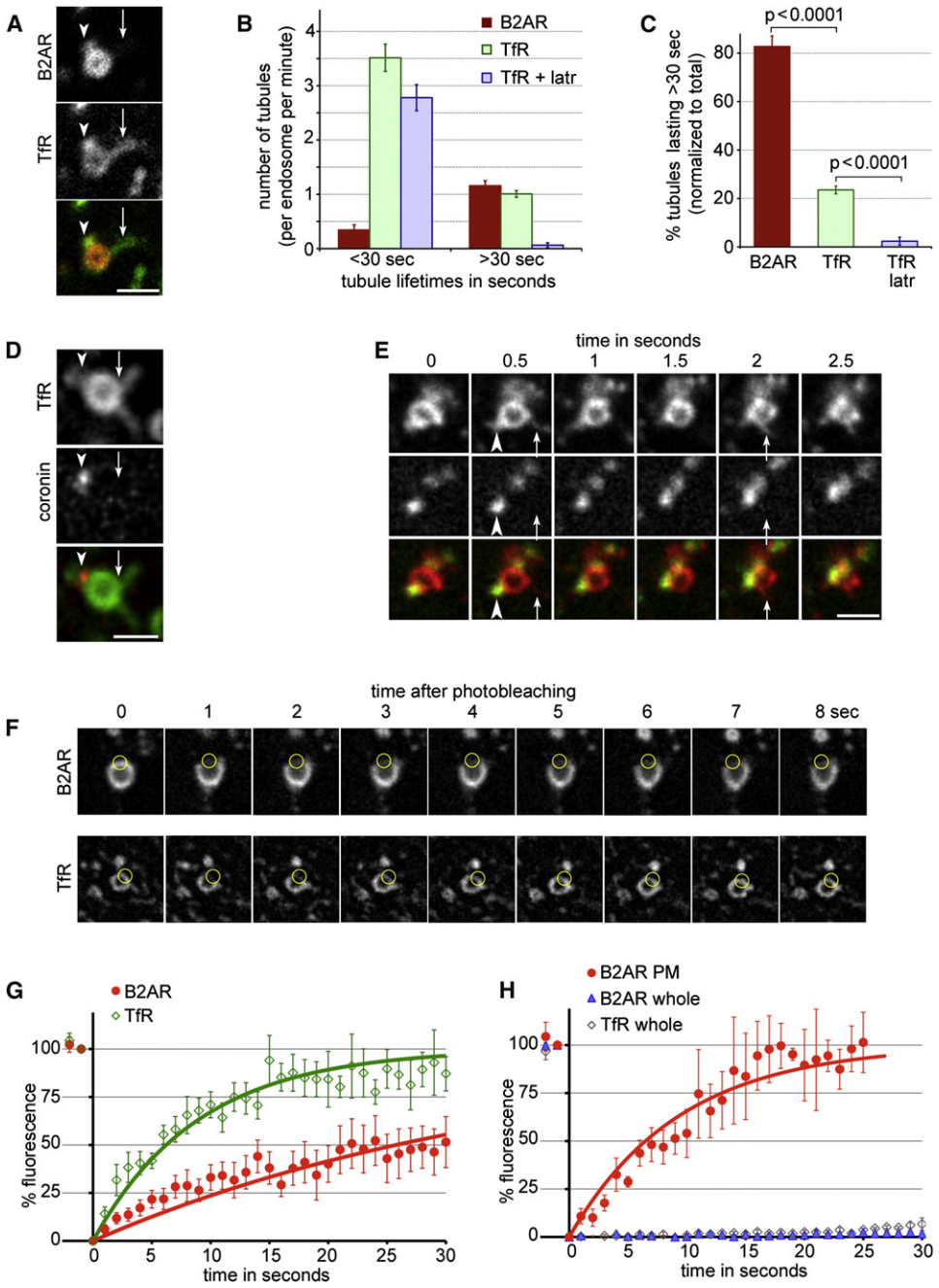

Figure 5. B2AR Is Enriched Specifically in a Subset of Endosomal Tubules that Are Stabilized by Actin

(A) A representative example of an endosome with two tubules containing TfR, only one of which is enriched for B2AR.

(B) The number of tubules with B2AR, TfR, and TfR in the presence of 10 μM latrunculin, per endosome per min, binned into lifetimes less than or more than 30 s, quantified across 28 endosomes and 281 tubules.

(C) The percentages of B2AR, TfR, and TfR + latrunculin tubules with lifetimes less than or more than 30 s, normalized to total number of tubules in each case.

(D) An example endosome containing TfR and coronin, showing that coronin is present on a subset of the TfR tubules. Arrowheads indicate a TfR tubule that is marked by coronin, and arrows show a TfR tubule that is not.

(E) Time lapse series showing TfR-containing tubules extruding from endosomal domains without detectable cortactin. Arrowheads indicate a relatively stable TfR tubule that is marked by coronin, and arrows denote rapid transient TfR tubules without detectable cortactin.

(F) Frames from a representative time lapse movie showing FRAP of B2AR (top row) or TfR (bottom row). The circles mark the bleached area of the endosome. TfR fluorescence recovers rapidly, while B2AR fluorescence recovers slowly.

(G) Fluorescence recovery of B2AR (red circles) and TfR (green diamonds) on endosomes quantified from 11 experiments. Exponential fits (solid lines) show that B2AR fluorescence recovers with a $t_{1/2}$ of 25.77 s ($R^2 = 0.83$, d.f = 37, Sy.x = 6.3), while TfR fluorescence recovers with a $t_{1/2}$ of 6.21 s ($R^2 = 0.91$, d.f = 30, Sy.x = 7.1).

PDZ-interacting recycling sequence on B2AR was both required and sufficient to mediate concentration of receptors in the actin-stabilized endosomal tubular domains.

As PDZ-domain interactions have been established to indirectly link various integral membrane proteins to cortical actin (Fehon et al., 2010), we tested whether linking DOR to actin was sufficient to drive receptor entry into endosomal tubules. Remarkably, fusion of the actin-binding domain of the ERM protein ezrin (Turunen et al., 1994) to the C terminus of DOR was sufficient to localize the receptor (termed DOR-ABD) to endosomal tubules (Figure 6J). The surface recycling of B2AR, DOR-B2, and DOR-ABD were dependent on the presence of an intact actin cytoskeleton (Figure S4), consistent with previous publications (Cao et al., 1999; Gage et al., 2005; Lauffer et al., 2009). Further, transplantation of the actin-binding domain was also sufficient to specifically confer recycling to a version of B2AR lacking its native recycling signal (Figure S4F). These results indicate that the concentration of B2AR in the actin-stabilized recycling tubules is mediated by linking receptors to the local actin cytoskeleton through PDZ interactions.

DISCUSSION

Even though endocytic receptor sorting was first appreciated over two decades ago (e.g., Brown et al., 1983; Farquhar, 1983; Steinman et al., 1983), our understanding of the principles of this process has been limited. A major reason for this has been the lack of direct assays to visualize signaling receptor sorting in the endosome. Here we directly visualized, in living cells, endosomal sorting between two prototypic members of the largest known family of signaling receptors for which sequence-specific recycling is critical for physiological regulation of cell signaling (Pippig et al., 1995; Lefkowitz et al., 1998; Xiang and Kobilka, 2003). We resolve sorting at the level of single trafficking events on individual endosomes, and define a kinetic and affinity-based model for how sequence-dependent receptors are sorted away from bulk-recycling and degrading proteins.

By analyzing individual sorting and recycling events on single endosomes, we demonstrate a remarkable diversity in recycling pathways emanating from the same organelle (Scita and Di Fiore, 2010). The traditional view has been that recycling to the plasma membrane is mediated by a uniform set of endosomal tubules from a single endosome. In contrast to this view, we demonstrate that the recycling pathway is highly specialized, and that specific cargo can segregate into specialized subsets of tubules that are biochemically, biophysically, and functionally distinct. Receptor recycling plays a critical role in controlling the rate of cellular re-sensitization to signals (Lefkowitz et al., 1998; Sorkin and von Zastrow, 2009), and recent data suggest that the sequence-dependent recycling of signaling receptors is selectively controlled by signaling pathways (Yudowski et al., 2009). The physical separation between bulk and sequence-dependent recycling that we demonstrate here allows for such selective control without affecting the recycling of constitutively cycling nutrient receptors. Further, such physical separation might also reflect the differences in molecular requirements that have been observed between bulk and sequence-dependent recycling (Hanyaloglu and von Zastrow, 2007).

Endosome-associated actin likely plays a dual role in endosomal sorting, both of which contribute to sequence-dependent entry of cargo selectively into special domains. First, by stabilizing the specialized endosomal tubules relative to the much more dynamic tubules that mediate bulk recycling, the local actin cytoskeleton could allow sequence-dependent cargo to overcome a kinetic barrier that limits their entry into the bulk pathway. Supporting this, we show that most endosomal tubules are highly transient, lasting less than a few seconds (Figures 5B and 5C), which allows enough time for entry of the fast-diffusing bulk recycling cargo, but not the slow-diffusing sequence-dependent cargo (Figures 5F and 5G), into these tubules. A subset of these tubules representing the sequence-dependent recycling pathway is stabilized by the presence of an actin cytoskeleton (Figures 5B and 5C). This stabilization allows time for B2AR to diffuse into these tubules (Figure S3), which eventually pinch off membranes that can directly fuse with the plasma membrane (Figure 2). Interestingly, inhibition of actin caused a decrease in the total number of tubules by approximately 25% (Figure 5B), suggesting that the actin cytoskeleton plays a role in maintaining the B2AR-containing subset of tubules, and not just in the sorting of B2AR into these tubules.

Second, a local actin cytoskeleton could provide the machinery for active concentration of recycling proteins like the B2AR, which interact with actin-associated sorting proteins (ERM and ERM-binding proteins) through C-terminal sequences (Weinman et al., 2006; Wheeler et al., 2007; Lauffer et al., 2009; Fehon et al., 2010), in specialized recycling tubules. Consistent with this, the C-terminal sequence on B2AR was both required and sufficient for sorting to the endosome and for recycling, and a distinct actin-binding sequence was sufficient for both receptor entry into tubules and recycling (Figure 6 and Figure S4). PDZ-interacting sequences have been identified on several signaling receptors, including multiple GPCRs, with different specificities for distinct PDZ-domain proteins (Weinman et al., 2006). Further, actin-stabilized subsets of tubules were present even in the absence of B2AR in the endosome. We propose that, using a combination of kinetic and affinity-based sorting principles, discrete Actin-Stabilized SEquence-dependent Recycling Tubule (ASSERT) domains could thus mediate efficient sorting of sequence-dependent recycling cargo away from both degradation and bulk recycling pathways that diverge from the same endosomes.

Our results, therefore, uncover an additional role for actin polymerization in endocytic sorting, separate from its role in endosome motility. It will be interesting to investigate the mechanism and signals that control the nucleation of such a spatially localized actin cytoskeleton on the endosome. The lack of obvious

(H) Fluorescence recovery of B2AR (blue triangles) and TfR (green diamonds) on endosomes when the whole endosome was bleached, or of B2AR on the cell surface (red circles) quantified from 12 experiments. B2AR fluorescence on the surface recovers with a $t_{1/2}$ of 6.49 s (R^2 = 0.94, d.f = 27, Sy.x = 8.1). Error bars denote SEM. Scale bars represent 1 μm. See also Figure S3 and Movie S8.

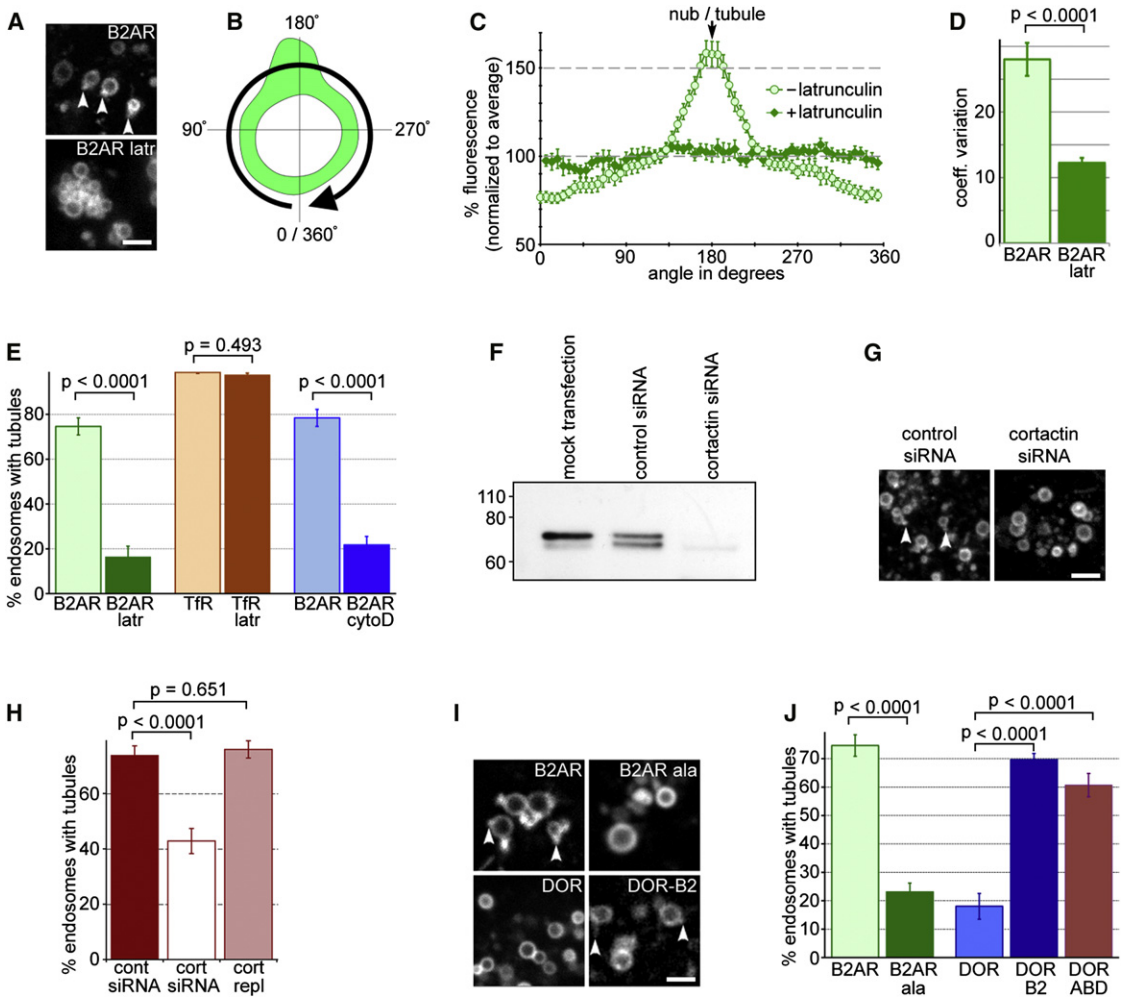

Figure 6. B2AR Enrichment in Tubules Depends on Endosomal Actin and a PDZ-Interacting Sequence on the B2AR Cytoplasmic Domain

(A) Representative fields from B2AR-expressing cells exposed to isoproterenol showing B2AR endosomes before (top panel) or after (bottom panel) exposure to 10 μM latrunculin for 5 min. Tubular endosomal domains enriched in B2AR (arrowheads) are lost upon exposure to latrunculin.

(B) Schematic of measurement of endosomal B2AR fluorescence profiles in the limiting membrane. The profile was measured in a clockwise manner starting from the area diametrically opposite the tubule (an angle of 0°).

(C) B2AR concentration along the endosomal membrane, calculated from fluorescence profiles of 20 endosomes, normalized to the average endosomal B2AR fluorescence. In the presence of latrunculin, B2AR enrichment in tubules is abolished, and B2AR fluorescence shows little variation along the endosomal membrane.

(D) Variance in endosomal B2AR fluorescence values measured before and after latrunculin. B2AR distribution becomes more uniform after latrunculin.

(E) The percentages of endosomes extruding B2AR-containing tubules, calculated before (n = 246) and after (n = 106) treatment with latrunculin, or before (n = 141) and after (n = 168) cytochalasin-D, show a significant reduction after treatment with either drug. As a control, the percentages of endosomes extruding TfR-containing tubules before (n = 317) and after (n = 286), respectively, are shown.

(F) Cortactin immunoblot showing reduction in protein levels after siRNA.

(G) Representative fields from B2AR-containing endosomes in cells treated with control and cortactin siRNA. Arrowheads denote endosomal tubules in the control siRNA-treated cells.

(H) Percentages of endosomes extruding B2AR tubules calculated in control siRNA-treated cells (n = 210), cortactin siRNA-treated cells (n = 269), and cortactin siRNA-treated cells expressing an siRNA-resistant cortactin (n = 250).

(I) Representative examples of endosomes from agonist-exposed cells expressing B2AR, B2AR-ala, DOR, or DOR-B2. Arrowheads denote receptor-containing tubules on B2AR and DOR-B2 endosomes.

(J) The percentage of endosomes with tubular domains containing B2AR, B2AR-ala, DOR, DOR-B2, or DOR-ABD (n = 246, 302, 137, 200, and 245, respectively) were quantified.

Scale bars represent 1 μm; and error bars represent SEM. See also Figure S4.

concentration of the canonical Arp2/3 activators, WASP and WAVE, suggests a novel mode of actin nucleation involving cortactin. Cortactin can act as a nucleation-promoting factor for Arp2/3, at least in vitro (Ammer and Weed, 2008), and can interact with dynamin (Schafer et al., 2002; McNiven et al., 2000), which makes it an attractive candidate for coordinating actin dynamics on membranes. Interestingly, inhibition of WASH, a recently described Arp regulator that is present on B2AR tubules, has been reported to result in an increase in endosomal tubules (Derivery et al., 2009). Although its role in sequence-dependent recycling remains to be tested, this suggests the presence of multiple actin-associated proteins with distinct functions on the endosome.

The simple kinetic and affinity-based principle that we propose likely provides a physical basis for sequence-dependent sorting of internalized membrane proteins between essentially opposite fates in distinct endosomal domains. Proteins that bind sequence-dependent degrading receptors and are required for their degradation (Whistler et al., 2002; Marley and von Zastrow, 2010) might act as scaffolds and provide a similar kinetic barrier to prevent them from accessing the rapid bulk-recycling tubules. Entry of these receptors into the involution pathway might then be accelerated by their association with the well-characterized ESCRT-associated domains on the vacuolar portion of endosomes (Hurley, 2008; Saksena et al., 2007; Williams and Urbé, 2007), complementary to the presently identified ASSERT domains on a subset of endosomal tubules.

Such diversity at the level of individual trafficking events to the same destination from the same organelle raises the possibility that there exists yet further specialization among the pathways that mediate exit out of the endosome, including in the degradative pathway and the retromer-based pathway to the trans-Golgi network. Importantly, the physical separation in pathways that we report here potentially allows for cargo-mediated regulation as a mode for controlling receptor recycling to the plasma membrane. Such a mechanism can provide virtually an unlimited level of selectivity in the post-endocytic system using minimal core trafficking machineries, as has been observed for endocytosis at the cell surface (Puthenveedu and von Zastrow, 2006). As the principles of such sorting depend critically on kinetics, the high-resolution imaging used here to analyze domain kinetics and biochemistry, and to achieve single-event resolution in living cells, provides a powerful method to elucidate biologically important sorting processes in the future.

EXPERIMENTAL PROCEDURES

Constructs and Reagents

Receptor constructs and stably transfected HEK293 cell lines are described previously (Gage et al., 2005; Lauffer et al., 2009) Transfections were performed using Effectene (QIAGEN) according to manufacturer's instructions. For visualizing receptors, FLAG-tagged receptors were labeled with M1 antibodies (Sigma) conjugated with Alexa-555 (Invitrogen) as described (Gage et al., 2005), or fusion constructs were generated where receptors were tagged on the N-terminus with GFP. Latrunculin and Cytochalasin D (Sigma) were used at 10 μM final concentration.

Live-Cell and Fluorescence Imaging

Cells were imaged using a Nikon TE-2000E inverted microscope with a 100× 1.49 NA TIRF objective (Nikon) and a Yokagawa CSU22 confocal head (Solamere), or an Andor Revolution XD Spinning disk system on a Nikon Ti microscope. A 488 nm Ar laser and a 568 nm Ar/Kr laser (Melles Griot), or 488 nm and 561 nm solid-state lasers (Coherent) were used as light sources. Cells were imaged in Opti-MEM (GIBCO) with 2% serum and 30 mM HEPES (pH 7.4), maintained at 37°C using a temperature-controlled incubation chamber. Time lapse images were acquired with a Cascade II EM-CCD camera (Photometrics) driven by MicroManager (www.micro-manager.org) or an Andor iXon+ EM-CCD camera using iQ (Andor). The same lasers were used as sources for bleaching in FRAP experiments. Structured illumination microscopy was performed as described earlier (Gustafsson et al., 2008).

Electron Microscopy

EM studies were carried out using MDCK cells because they are amenable to a previously described pre-embedding processing that facilitates detection of cytoplasmic actin filaments (Ikonen et al., 1996; Parton et al., 1991), and because they contain morphologically similar endosomes to HEK293 cells. Cells were grown on polycarbonate filters (Transwell 3412; Costar, Cambridge, MA) for 4 days as described previously (Parton et al., 1991). To allow visualization of early endosomes and any associated filaments a pre-embedding approach was employed. Cells were incubated with HRP (Sigma type II, 10mg/ml) in the apical and basolateral medium for 10min at 37°C and then washed, perforated, and immunogold labeled with a rabbit anti- actin antibody, a gift of Professor Jan de Mey (Strasbourg), followed by 9nm protein A-gold. HRP visualization and epon embedding was as described previously (Parton et al., 1991; Ikonen et al., 1996).

Image and Data Analysis

Acquired image sequences were saved as 16-bit tiff stacks, and quantified using ImageJ (http://rsb.info.nih.gov/ij/). For estimating receptor enrichment, a circular mask 5 px in diameter was used to manually select the membrane at the base of the tubule or membranes derived from endosomes. Fluorescence values measured were normalized to that of the endosomal membrane devoid of tubules. An area of the coverslip lacking cells was used to estimate background fluorescence. For estimating linear pixel values along the tubules, a line selection was drawn along the tubule and across the endosome, and the Plot Profile function used to measure pixel values. For obtaining the average value plot across multiple sorting events, the linear pixels were first normalized to the diameter of the endosome and then averaged. To generate pixel values along the endosomal limiting membranes, the Oval Profile plugin, with 60 segments, was used after manually selecting the endosomal membrane using an oval ROI. Lifetimes of tubules were calculated by manually tracking the extension and retraction of tubules over time-lapse series. Microsoft Excel was used for simple data analyses and graphing. Curve fits of data were performed using GraphPad Prism. All P-values are from two-tailed Mann-Whitney tests unless otherwise noted.

SUPPLEMENTAL INFORMATION

Supplemental Information includes four figures and eight movies and can be found with this article online at doi:10.1016/j.cell.2010.10.003.

ACKNOWLEDGMENTS

The majority of the imaging was performed at the Nikon Imaging Center at UCSF. We thank David Drubin, Matt Welch, John Sedat, Aylin Hanyaloglu, Aaron Marley, and James Hislop for essential reagents and valuable help. M.A.P. was supported by a K99/R00 grant DA024698, M.v.Z. by an R37 grant DA010711, and O.D.W. by an RO1 grant GM084040, all from the NIH. J.T. is an investigator of the Howard Hughes Medical Institute.

Received: October 31, 2009
Revised: April 7, 2010
Accepted: September 27, 2010
Published: November 24, 2010

REFERENCES

Ammer, A.G., and Weed, S.A. (2008). Cortactin branches out: roles in regulating protrusive actin dynamics. Cell Motil. Cytoskeleton *65*, 687–707.

Brown, M.S., Anderson, R.G., and Goldstein, J.L. (1983). Recycling receptors: the round-trip itinerary of migrant membrane proteins. Cell *32*, 663–667.

Benink, H.A., and Bement, W.M. (2005). Concentric zones of active RhoA and Cdc42 around single cell wounds. J. Cell Biol. *168*, 429–439.

Cao, T.T., Deacon, H.W., Reczek, D., Bretscher, A., and von Zastrow, M. (1999). A kinase-regulated PDZ-domain interaction controls endocytic sorting of the β2-adrenergic receptor. Nature *401*, 286–290.

Cullen, P.J. (2008). Endosomal sorting and signalling: an emerging role for sorting nexins. Nat. Rev. Mol. Cell Biol. *9*, 574–582.

Daly, R.J. (2004). Cortactin signalling and dynamic actin networks. Biochem. J. *382*, 13–25.

Derivery, E., Sousa, C., Gautier, J.J., Lombard, B., Loew, D., and Gautreau, A. (2009). The Arp2/3 activator WASH controls the fission of endosomes through a large multiprotein complex. Dev. Cell *17*, 712–723.

Duleh, S.N., and Welch, M.D. (2010). WASH and the Arp2/3 complex regulate endosome shape and trafficking. Cytoskeleton (Hoboken) *67*, 193–206.

Dunn, K.W., and Maxfield, F.R. (1992). Delivery of ligands from sorting endosomes to late endosomes occurs by maturation of sorting endosomes. J. Cell Biol. *117*, 301–310.

Farquhar, M.G. (1983). Intracellular membrane traffic: pathways, carriers, and sorting devices. Methods Enzymol. *98*, 1–13.

Fehon, R.G., McClatchey, A.I., and Bretscher, A. (2010). Organizing the cell cortex: the role of ERM proteins. Nat. Rev. Mol. Cell Biol. *11*, 276–287.

Gage, R.M., Matveeva, E.A., Whiteheart, S.W., and von Zastrow, M. (2005). Type I PDZ ligands are sufficient to promote rapid recycling of G Protein-coupled receptors independent of binding to N-ethylmaleimide-sensitive factor. J. Biol. Chem. *280*, 3305–3313.

Girao, H., Geli, M.I., and Idrissi, F.Z. (2008). Actin in the endocytic pathway: from yeast to mammals. FEBS Lett. *582*, 2112–2119.

Gomez, T.S., and Billadeau, D.D. (2009). A FAM21-containing WASH complex regulates retromer-dependent sorting. Dev. Cell *17*, 699–711.

Gustafsson, M.G., Shao, L., Carlton, P.M., Wang, C.J., Golubovskaya, I.N., Cande, W.Z., Agard, D.A., and Sedat, J.W. (2008). Three-dimensional resolution doubling in wide-field fluorescence microscopy by structured illumination. Biophys. J. *94*, 4957–4970.

Hanyaloglu, A.C., and von Zastrow, M. (2007). A novel sorting sequence in the beta2-adrenergic receptor switches recycling from default to the Hrs-dependent mechanism. J. Biol. Chem. *282*, 3095–3104.

Hanyaloglu, A.C., and von Zastrow, M. (2008). Regulation of GPCRs by endocytic membrane trafficking and its potential implications. Annu. Rev. Pharmacol. Toxicol. *48*, 537–568.

Hanyaloglu, A.C., McCullagh, E., and von Zastrow, M. (2005). Essential role of Hrs in a recycling mechanism mediating functional resensitization of cell signaling. EMBO J. *24*, 2265–2283.

Hurley, J.H. (2008). ESCRT complexes and the biogenesis of multivesicular bodies. Curr. Opin. Cell Biol. *20*, 4–11.

Ikonen, E., Parton, R.G., Lafont, F., and Simons, K. (1996). Analysis of the role of p200-containing vesicles in post-Golgi traffic. Mol. Biol. Cell *7*, 961–974.

Kaksonen, M., Peng, H.B., and Rauvala, H. (2000). Association of cortactin with dynamic actin in lamellipodia and on endosomal vesicles. J. Cell Sci. *113*, 4421–4426.

Kaksonen, M., Toret, C.P., and Drubin, D.G. (2005). A modular design for the clathrin- and actin-mediated endocytosis machinery. Cell *123*, 305–320.

Lauffer, B.E., Chen, S., Melero, C., Kortemme, T., von Zastrow, M., and Vargas, G.A. (2009). Engineered protein connectivity to actin mimics PDZ-dependent recycling of G protein-coupled receptors but not its regulation by Hrs. J. Biol. Chem. *284*, 2448–2458.

Lefkowitz, R.J., Pitcher, J., Krueger, K., and Daaka, Y. (1998). Mechanisms of beta-adrenergic receptor desensitization and resensitization. Adv. Pharmacol. *42*, 416–420.

Marchese, A., Paing, M.M., Temple, B.R., and Trejo, J. (2008). G protein-coupled receptor sorting to endosomes and lysosomes. Annu. Rev. Pharmacol. Toxicol. *48*, 601–629.

Marley, A., and von Zastrow, M. (2010). Dysbindin promotes the post-endocytic sorting of G protein-coupled receptors to lysosomes. PLoS ONE *5*, e9325.

Maxfield, F.R., and McGraw, T.E. (2004). Endocytic recycling. Nat. Rev. Mol. Cell Biol. *5*, 121–132.

Mayor, S., Presley, J.F., and Maxfield, F.R. (1993). Sorting of membrane components from endosomes and subsequent recycling to the cell surface occurs by a bulk flow process. J. Cell Biol. *121*, 1257–1269.

McNiven, M.A., Kim, L., Krueger, E.W., Orth, J.D., Cao, H., and Wong, T.W. (2000). Regulated interactions between dynamin and the actin-binding protein cortactin modulate cell shape. J. Cell Biol. *151*, 187–198.

Merrifield, C.J., Qualmann, B., Kessels, M.M., and Almers, W. (2004). Neural Wiskott Aldrich Syndrome Protein (N-WASP) and the Arp2/3 complex are recruited to sites of clathrin-mediated endocytosis in cultured fibroblasts. Eur. J. Cell Biol. *83*, 13–18.

Miesenböck, G., De Angelis, D.A., and Rothman, J.E. (1998). Visualizing secretion and synaptic transmission with pH-sensitive green fluorescent proteins. Nature *394*, 192–195.

Millard, T.H., Sharp, S.J., and Machesky, L.M. (2004). Signalling to actin assembly via the WASP (Wiskott-Aldrich syndrome protein)-family proteins and the Arp2/3 complex. Biochem. J. *380*, 1–17.

Parton, R.G., Dotti, C.G., Bacallao, R., Kurtz, I., Simons, K., and Prydz, K. (1991). pH-induced microtubule-dependent redistribution of late endosomes in neuronal and epithelial cells. J. Cell Biol. *113*, 261–274.

Perrais, D., and Merrifield, C.J. (2005). Dynamics of endocytic vesicle creation. Dev. Cell *9*, 581–592.

Piper, R.C., and Katzmann, D.J. (2007). Biogenesis and function of multivesicular bodies. Annu. Rev. Cell Dev. Biol. *23*, 519–547.

Pippig, S., Andexinger, S., and Lohse, M.J. (1995). Sequestration and recycling of beta 2-adrenergic receptors permit receptor resensitization. Mol. Pharmacol. *47*, 666–676.

Pollard, T.D. (2007). Regulation of actin filament assembly by Arp2/3 complex and formins. Annu. Rev. Biophys. Biomol. Struct. *36*, 451–477.

Puthenveedu, M.A., and von Zastrow, M. (2006). Cargo regulates clathrin-coated pit dynamics. Cell *127*, 113–124.

Saksena, S., Sun, J., Chu, T., and Emr, S.D. (2007). ESCRTing proteins in the endocytic pathway. Trends Biochem. Sci. *32*, 561–573.

Schafer, D.A., Weed, S.A., Binns, D., Karginov, A.V., Parsons, J.T., and Cooper, J.A. (2002). Dynamin2 and cortactin regulate actin assembly and filament organization. Curr. Biol. *12*, 1852–1857.

Scita, G., and Di Fiore, P.P. (2010). The endocytic matrix. Nature *463*, 464–473.

Shinozaki-Narikawa, N., Kodama, T., and Shibasaki, Y. (2006). Cooperation of phosphoinositides and BAR domain proteins in endosomal tubulation. Traffic *7*, 1539–1550.

Sorkin, A., and von Zastrow, M. (2009). Endocytosis and signalling: intertwining molecular networks. Nat. Rev. Mol. Cell Biol. *10*, 609–622.

Stamnes, M. (2002). Regulating the actin cytoskeleton during vesicular transport. Curr. Opin. Cell Biol. *14*, 428–433.

Steinman, R.M., Mellman, I.S., Muller, W.A., and Cohn, Z.A. (1983). Endocytosis and the recycling of plasma membrane. J. Cell Biol. *96*, 1–27.

Traer, C.J., Rutherford, A.C., Palmer, K.J., Wassmer, T., Oakley, J., Attar, N., Carlton, J.G., Kremerskothen, J., Stephens, D.J., and Cullen, P.J. (2007). SNX4 coordinates endosomal sorting of TfnR with dynein-mediated transport into the endocytic recycling compartment. Nat. Cell Biol. *9*, 1370–1380.

Turunen, O., Wahlström, T., and Vaheri, A. (1994). Ezrin has a COOH-terminal actin-binding site that is conserved in the ezrin protein family. J. Cell Biol. *126*, 1445–1453.

Uetrecht, A.C., and Bear, J.E. (2006). Coronins: the return of the crown. Trends Cell Biol. *16*, 421–426.

Weinman, E.J., Hall, R.A., Friedman, P.A., Liu-Chen, L.Y., and Shenolikar, S. (2006). The association of NHERF adaptor proteins with g protein-coupled receptors and receptor tyrosine kinases. Annu. Rev. Physiol. *68*, 491–505.

Wheeler, D., Sneddon, W.B., Wang, B., Friedman, P.A., and Romero, G. (2007). NHERF-1 and the cytoskeleton regulate the traffic and membrane dynamics of G protein-coupled receptors. J. Biol. Chem. *282*, 25076–25087.

Whistler, J.L., Enquist, J., Marley, A., Fong, J., Gladher, F., Tsuruda, P., Murray, S.R., and Von Zastrow, M. (2002). Modulation of postendocytic sorting of G protein-coupled receptors. Science *297*, 615–620.

Williams, R.L., and Urbé, S. (2007). The emerging shape of the ESCRT machinery. Nat. Rev. Mol. Cell Biol. *8*, 355–368.

Xiang, Y., and Kobilka, B.K. (2003). Myocyte adrenoceptor signaling pathways. Science *300*, 1530–1532.

Yarar, D., Waterman-Storer, C.M., and Schmid, S.L. (2005). A dynamic actin cytoskeleton functions at multiple stages of clathrin-mediated endocytosis. Mol. Biol. Cell *16*, 964–975.

Yudowski, G.A., Puthenveedu, M.A., and von Zastrow, M. (2006). Distinct modes of regulated receptor insertion to the somatodendritic plasma membrane. Nat. Neurosci. *9*, 622–627.

Yudowski, G.A., Puthenveedu, M.A., Henry, A.G., and von Zastrow, M. (2009). Cargo-mediated regulation of a rapid Rab4-dependent recycling pathway. Mol. Biol. Cell *20*, 2774–2784.

Zerial, M., and McBride, H. (2001). Rab proteins as membrane organizers. Nat. Rev. Mol. Cell Biol. *2*, 107–117.